

| | |
|-----------------------------|---|
| Title | On thermodynamics in the primary power conversion of oscillating water column wave energy converters |
| Authors | Sheng, Wanan;Alcorn, Raymond;Lewis, Anthony |
| Publication date | 2013-03-06 |
| Original Citation | Sheng, W., Alcorn, R. and Lewis, A. (2013) 'On thermodynamics in the primary power conversion of oscillating water column wave energy converters' Journal of Renewable and Sustainable Energy, 5, 023105. http://dx.doi.org/10.1063/1.4794750 |
| Type of publication | Article (peer-reviewed) |
| Link to publisher's version | 10.1063/1.4794750 |
| Rights | © 2013 American Institute of Physics. This article may be downloaded for personal use only. Any other use requires prior permission of the author and AIP Publishing. The following article appeared in Sheng et al., Journal of Renewable and Sustainable Energy, 5, 023105 (2013) and may be found at http://dx.doi.org/10.1063/1.4794750 |
| Download date | 2024-04-28 03:45:39 |
| Item downloaded from | https://hdl.handle.net/10468/2691 |

On thermodynamics in the primary power conversion of oscillating water column wave energy converters

Wanan Sheng, Raymond Alcorn, and Anthony Lewis

Citation: *J. Renewable Sustainable Energy* **5**, 023105 (2013); doi: 10.1063/1.4794750

View online: <http://dx.doi.org/10.1063/1.4794750>

View Table of Contents: <http://jrse.aip.org/resource/1/JRSEBH/v5/i2>

Published by the [American Institute of Physics](#).

Related Articles

Feasibility analysis and proof of concept for thermoelectric energy harvesting in mobile computers

J. Renewable Sustainable Energy **5**, 023103 (2013)

An integrated inductor for high current with using Fe-Si metal alloy composite films

J. Appl. Phys. **113**, 17A302 (2013)

A new kind of low-inductance transformer type magnetic switch (TTMS) with coaxial cylindrical conductors

Rev. Sci. Instrum. **84**, 023306 (2013)

Cross-correlation detection and analysis for California's electricity market based on analogous multifractal analysis

Chaos **23**, 013129 (2013)

Disintegration of rocks based on magnetically isolated high voltage discharge

Rev. Sci. Instrum. **84**, 024704 (2013)

Additional information on J. Renewable Sustainable Energy

Journal Homepage: <http://jrse.aip.org/>

Journal Information: http://jrse.aip.org/about/about_the_journal

Top downloads: http://jrse.aip.org/features/most_downloaded

Information for Authors: <http://jrse.aip.org/authors>

ADVERTISEMENT

AIP | Journal of Renewable and Sustainable Energy

Sign Up For the Free Newsletter Today!

AIP | Journal of Renewable and Sustainable Energy



On thermodynamics in the primary power conversion of oscillating water column wave energy converters

Wanan Sheng, Raymond Alcorn, and Anthony Lewis

Hydraulics and Maritime Research Centre, University College Cork, Cork, Ireland

(Received 19 November 2012; accepted 22 February 2013; published online 6 March 2013)

The paper presents an investigation to the thermodynamics of the air flow in the air chamber for the oscillating water column wave energy converters, in which the oscillating water surface in the water column pressurizes or de-pressurizes the air in the chamber. To study the thermodynamics and the compressibility of the air in the chamber, a method is developed in this research: the power take-off is replaced with an accepted semi-empirical relationship between the air flow rate and the oscillating water column chamber pressure, and the thermodynamic process is simplified as an isentropic process. This facilitates the use of a direct expression for the work done on the power take-off by the flowing air and the generation of a single differential equation that defines the thermodynamic process occurring inside the air chamber. Solving the differential equation, the chamber pressure can be obtained if the interior water surface motion is known or the chamber volume (thus the interior water surface motion) if the chamber pressure is known. As a result, the effects of the air compressibility can be studied. Examples given in the paper have shown the compressibility, and its effects on the power losses for large oscillating water column devices. © 2013 American Institute of Physics.

[<http://dx.doi.org/10.1063/1.4794750>]

NOMENCLATURE

| | |
|------------------|--|
| A_0, A_1 | area of water column and orifice |
| C_q | flow coefficient through orifice |
| E_p | power deficiency due to air compressibility |
| k_1, k_2 | linear and nonlinear flowrate damping coefficients |
| m | air mass in the air chamber |
| p, p_0, p_c | chamber gauge pressure ("chamber pressure" hereafter), atmospheric pressure, absolute chamber pressure |
| P_{pto}, P_w | power to PTO system and power generated by wave |
| Q_p, Q_w | flowrate through PTO and driven by water surface, respectively |
| T, T_0, T_c | temperature (fluctuation, atmospheric and absolute temperature in chamber) |
| V, V_0 | air volume (time dependent) and air volume in calm water |
| x | interior water surface motion |
| ρ_0, ρ_c | atmospheric and chamber air density |
| γ | specific heat ratio of air ($\gamma = 1.4$) |
| BBDB | backward bend duct buoy |
| DOF | degree of freedom |
| ECN | Ecole Centrale de Nantes (France) |
| HMRC | Hydraulics and Maritime Research Centre (Ireland) |
| IWS | interior water surface |
| OWC | oscillating water column |
| PTO | power take-off |
| WEC | wave energy converter |
| LHS/RHS | left/right hand side |

Subscripts

| | |
|-----|-----------------------------------|
| L | large model for an upscaled model |
| m | model |
| c | value in air chamber |
| 0 | constant or atmospheric value |

I. INTRODUCTION

As one type of most successful wave energy converters (WECs), oscillating water column (OWC) WECs have been studied through a quite long period of development and research, and their technologies are relatively mature when compared to other wave energy converters. Practically, some OWC wave power plants have so far been built and generated electricity to the grid, for example, LIMPET in Scotland¹ and PICO in Portugal.² Now floating OWC WECs are getting more and more popular due to their possible deployment in the open and deeper water regions, where a large wave energy resource is available. Wavegen commissioned by DTI³ has conducted a comparison study on three different types of floating OWCs, namely the spar OWC, the backward bend duct buoy (BBDB) OWC, and the sloped OWC, sketched in Figure 1. More studies on this topic can be found in Refs. 4–10.

Generally, OWC WECs have many advantages over other wave energy converters in terms of (i) a confirmed concept; several practical OWC plants have been built and actually generated electricity to the grids; (ii) an adaptive device, either fixed on shoreline or on seabed or floating in waves; (iii) a device with a relatively high “wave-to-wire” energy conversion efficiency, including a high primary energy conversion efficiency, and a relatively high mechanical power converting efficiency; (iv) no moving component in sea water; (v) more importantly, a small force/torque and a high speed for a certain power take-off (PTO), such that the reliability of the PTO system should be guaranteed; (vi) a relative small motion of the structure or even a fixed structure for wave energy conversion.

Theoretical work on the hydrodynamic performance of OWCs has progressed significantly in the past two decades. Evans¹¹ and Evans and Porter¹² studied the OWC system theoretically by employing potential theory, and worked out that its maximum power take-off by OWC can be 100%. Lee *et al.*^{13,14} have further studied OWC numerically, and extended their boundary element method code WAMIT¹⁵ by including the generalized modes to the conventional 6-degree of freedom (DOF) motions in such a way that the independent motions of the interior water surface (IWS) can be easily included and analysed by simply specifying the relevant normal velocities on the interested boundaries. Hong *et al.*^{4,5} gave a detailed derivation of the potential theory for floating OWC wave energy converters by including an assumed linear air flow through a duct/orifice. In all these studies, incompressible air is assumed. More recently,

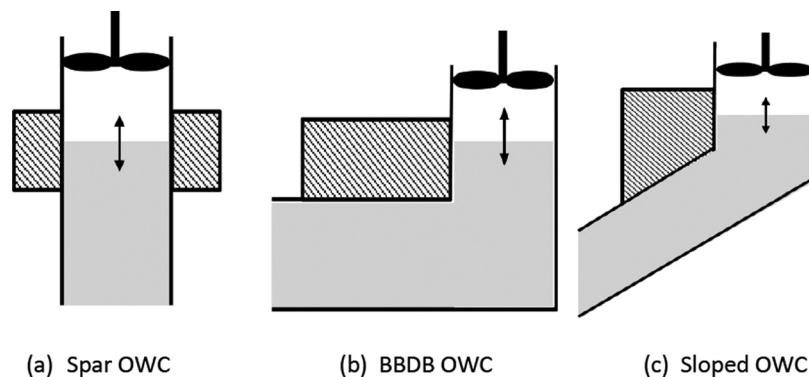


FIG. 1. Floating OWC WECs.

Nagata *et al.*¹⁰ divided the whole flow region into two coupled regions: one region represents the external flow field, and the other the flow field in the OWC water column. These two regions are coupled via their sharing surface to form a full dynamic system.

Relatively, the thermodynamics of air in the air chamber, including the effect of air compressibility, has been studied by few researchers. Sarmento *et al.*¹⁶ first put forward a formula for the air compressibility under the assumption of a large volume of the air chamber (compare to the air volume changes). This equation has been widely accepted and used by other researchers.^{17,18} Josset and Clément¹⁹ presented a time-domain approach for the foundation-type OWC plants, in which the flow field has been divided into two sub-problems: interior and external problems. In the simulation, the external problem, being solved only once, couples the interior problems via a common surface. Besides, the interior problem is also coupled with the thermodynamics and a linear power take-off. Falcao *et al.*²⁰ studied the air flow control to improve the overall efficiency of the OWC devices, and pointed out there are significant differences between the air inhalation and exhalation processes. In exhalation, the pressurized air passes through the PTO system with a larger density than that of atmosphere, and a complicated air mixing process happens at the outside of the air chamber. Essentially, the air in air chamber remains uniform and smooth. In contrast, in the process of air inhalation, the air in the air chamber is de-pressurised, and its density and temperature are lower than those in the atmosphere. When the atmosphere is inhaled in, the air mixing process occurs in the air chamber and is much more complicated for study. To simplify the analysis, the air mixing process is normally assumed to be instant. This may be accepted due to the fact of the slow reciprocations of the interior water surface motion.

Further, the air is considered as an isentropic gas in an open thermodynamic system.^{10,16–21} The mass and energy exchanges happen only through the open boundaries (the interior water surface and the PTO). For instance, the work is done to the air in the chamber by the interior water surface motion, and the work is done to the PTO system by the mass flow through the PTO. Due to the dependence of the energy passed to the PTO on the mass exchange across the open boundary, compressibility may lead to a drop in a small portion of the system energy that is extracted from the waves for power generation.

To study the effects of air compressibility in the chamber, a method is proposed in this paper that is based on the assumptions which are similar to the existing procedure of Sarmento *et al.*,¹⁶ and by applying the known PTO characteristics, an ordinary differential equation has been derived for the chamber pressure and the chamber volume (and thus the flowrate). Solving the ordinary differential equation, the effects of the air compressibility can be obtained. For an application of the proposed method, a small test model of an OWC device is scaled up for studying the effects of air compressibility. In the example, the interior water surface motion in the upscaled device is assumed to be known and the chamber pressure is then obtained by solving the thermodynamic differential equation. It can be seen that air compressibility is clearly shown for a large OWC device, and due to the compressibility, a power loss is also induced.

II. THERMODYNAMICS OF OWC

The uniformity of the air in the air chamber is assumed regardless of the processes of exhalation and inhalation. Under the assumption, the air state can be expressed by the uniformity parameters, such as pressure, p_c , density, ρ_c , and temperature T_c in the chamber (see Figure 2). The absolute chamber pressure and the air temperature can be taken as their fluctuations, p (the gauge chamber pressure, or the chamber pressure hereafter) and T , superimposed to the corresponding atmospheric values denoted with a subscript 0, as

$$\begin{cases} p_c = p_0 + p \\ T_c = T_0 + T. \end{cases} \quad (1)$$

The dynamic system considered in the research is an open thermodynamic system, and the control volume is enclosed by the water column walls, an opening to the PTO, and an open boundary (i.e., the IWS). The PTO is regarded as a thin disc with a pressure drop across it. This

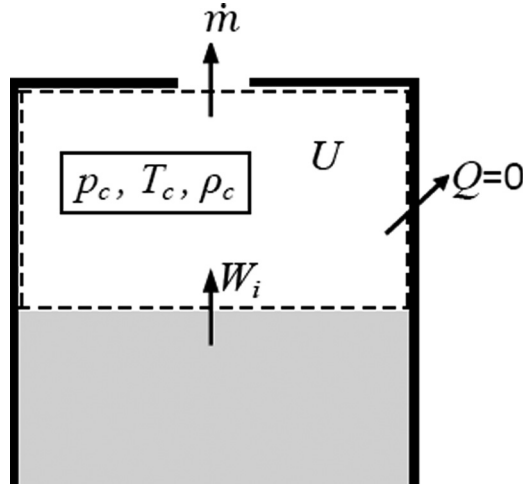


FIG. 2. The OWC chamber and the control volume (dashed lines).

simplification excludes the study of the detailed flow through the PTO device, for example, an air turbine.

Through the open PTO boundary, an air mass flow is created during the exhalation and inhalation. The mass flow provides the PTO an available pneumatic power, defined as the chamber pressure multiplying the flowrate through the PTO. The mass flow drives the PTO system to extract the pneumatic energy from the chamber to useful mechanical energy.

Through the IWS open boundary, the wave does work, W_i , to the thermodynamic system, part of which is the wave supplied pneumatic work, defined as the chamber pressure multiplying by the volume change rate.

For the open system, the first thermodynamic law can be expressed as (following Ref. 19)

$$\frac{d(mc_v T_c)}{dt} = -p_c \frac{dV}{dt} + c_p T_c \dot{m} - \dot{Q}, \quad (2)$$

where the LHS term is the changing rate of the internal energy in the control volume; the first term in the RHS is the wave excited power to the system; the second term in the RHS is the rate of the energy exchange through the open PTO boundary, while \dot{Q} is the heat exchange through the walls. In this study, $\dot{Q} = 0$ for the adiabatic process.

The mass of air in the chamber can be expressed as

$$m = \rho_c V, \quad (3)$$

where m is the time dependent air mass in the air chamber, V the air volume of the chamber.

The flow rate driven by the water surface is simply expressed (see Ref. 16) as

$$\dot{Q}_w = -\frac{dV}{dt}. \quad (4)$$

Differentiating Eq. (3) gives

$$\frac{dm}{dt} = \rho_c \frac{dV}{dt} + V \frac{d\rho_c}{dt}. \quad (5)$$

It must be noted that a positive value of the mass rate means some air is inhaled in to the chamber through the PTO system (inhalation), and a negative value of the mass rate means some air is driven out of the air chamber (exhalation).

Exhalation happens when the chamber pressure is larger than the atmospheric pressure, during which the air in the air chamber is pressurized so that some air is exhaled from the air chamber. The condition for exhalation is

$$p > 0. \quad (6a)$$

Inhalation happens when the chamber pressure is smaller than the atmospheric pressure, during which the air is de-compressed in the air chamber, thus some air is inhaled into the chamber through the power take-off system. The condition for inhalation is

$$p < 0. \quad (6b)$$

Due to compressibility, the air density can change in the air chamber during exhalation and inhalation. In exhalation, the pressurized air is driven out through the power take-off system, while in inhalation, the atmosphere is inhaled in through the power take-off system. Thus, the air volume flowrate must be considered for exhalation and inhalation differently due to the air flow through the PTO with different densities,

$$\begin{cases} Q_p = -\frac{1}{\rho_c} \frac{dm}{dt}, & \text{for exhalation} \\ Q_p = -\frac{1}{\rho_0} \frac{dm}{dt}, & \text{for inhalation.} \end{cases} \quad (7)$$

Based on the air flowrates generated by the water surface, the input power in the OWC converter is calculated by the chamber pressure multiplying the flow rate driven by the water surface, as

$$P_w = pQ_w. \quad (8)$$

Correspondingly, the output power available to the PTO system is

$$P_{pto} = pQ_p. \quad (9)$$

A. Incompressible air

A simple case is for the incompressible air, which may occur in small scale model, when its pressure and air volume are both small. Due to the incompressibility of the air, the air density and temperature in the air chamber are constants, same as those of atmospheric values. Under such an assumption, the air mass in the air chamber can be simply expressed as

$$m = \rho_0 V, \quad (10)$$

in which the mass change rate is purely caused by the change of the air volume, and the flow rate through the power take-off system is

$$Q_p = -\frac{1}{\rho_0} \frac{dm}{dt} = -\frac{dV}{dt} = Q_w. \quad (11)$$

It can be seen that the flowrate driven by the interior water surface in the OWC water column is completely through the power take-off system, ensuring,

$$P_{pto} = P_w. \quad (12)$$

Hence, for incompressible air, the wave generated power is fully transferred to the power take-off system.

B. Ideal air

To simplify the thermodynamic problem of the OWC wave energy converter, the air in the chamber is considered as isentropic, which gives a state equation for the open system of the air chamber as,

$$\frac{p_c}{\rho_c^\gamma} = \text{constant}, \quad (13)$$

where γ is the specific heat ratio of the air ($\gamma = 1.4$).

Equation (13) can be also expressed as

$$\frac{p_0 + p}{\rho_c^\gamma} = \frac{p_0}{\rho_0^\gamma}. \quad (14)$$

So

$$\rho_c = \rho_0 \left(1 + \frac{p}{p_0} \right)^{\frac{1}{\gamma}}. \quad (15)$$

A linearised form of Eq. (15) if $|p|$ is much smaller than p_0 .

$$\rho_c = \rho_0 \left(1 + \frac{p}{\gamma p_0} \right). \quad (16)$$

The air density in the chamber is linear with the chamber pressure. Figure 3 gives the comparison between Eqs. (15) and (16), and it can be seen that the linearised version (16) represents formula (15) very well, and up to a pressure of 15 000 Pa (a very high pressure in the air chamber for OWC devices), there is an error of less than 0.2%. Hence, the linearised density expression is a very good approximation, and will be used hereafter.

Similarly, the temperature changes due to the changes of the pressure in the chamber, given by an equation,

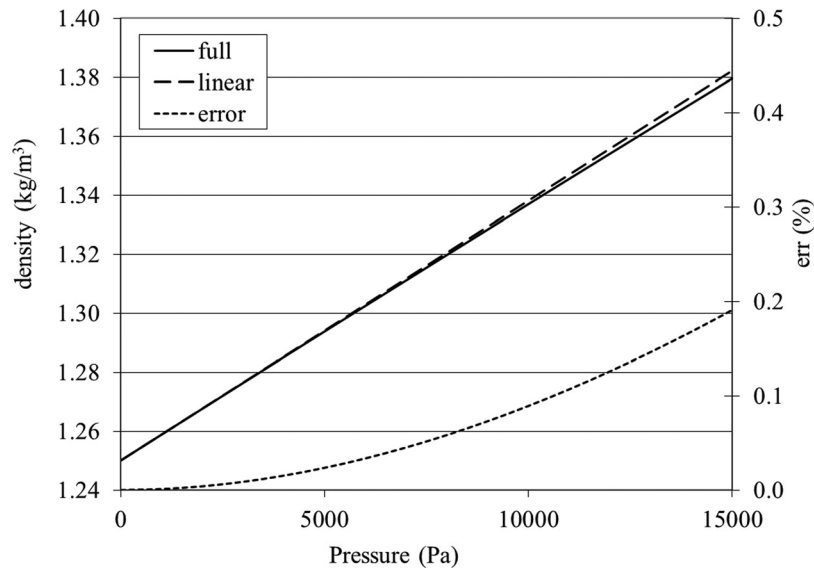


FIG. 3. Air density in the air chamber for different chamber pressures.

$$T_c p_c^{\frac{1-\gamma}{\gamma}} = \text{constant}. \quad (17)$$

So

$$T_c = T_0 \left(1 + \frac{p}{p_0} \right)^{\frac{\gamma-1}{\gamma}} \quad (18)$$

and its linearised form is

$$T_c = T_0 \left(1 + \frac{\gamma-1}{\gamma} \frac{p}{p_0} \right). \quad (19)$$

Correspondingly, the chamber temperature is calculated as

$$T = T_0 \frac{\gamma-1}{\gamma} \frac{p}{p_0}. \quad (20)$$

Again, the air temperature in the chamber is linear with the chamber pressure. Figure 4 gives the comparison between Eqs. (18) and (19), and it can be seen that the linearised version (19) represents formula (18) very well, and there is an error of $<0.2\%$ for a pressure up to 15 000 Pa.

From Eq. (16), its differential form is

$$\frac{d\rho_c}{dt} = \frac{\rho_0}{\gamma p_0} \frac{dp}{dt}. \quad (21)$$

Substituting Eqs. (5), (16), and (21) into (7) yields

$$Q_p = Q_w - \frac{V}{\gamma p_0 + p} \frac{dp}{dt} \quad (\text{exhalation}), \quad (22a)$$

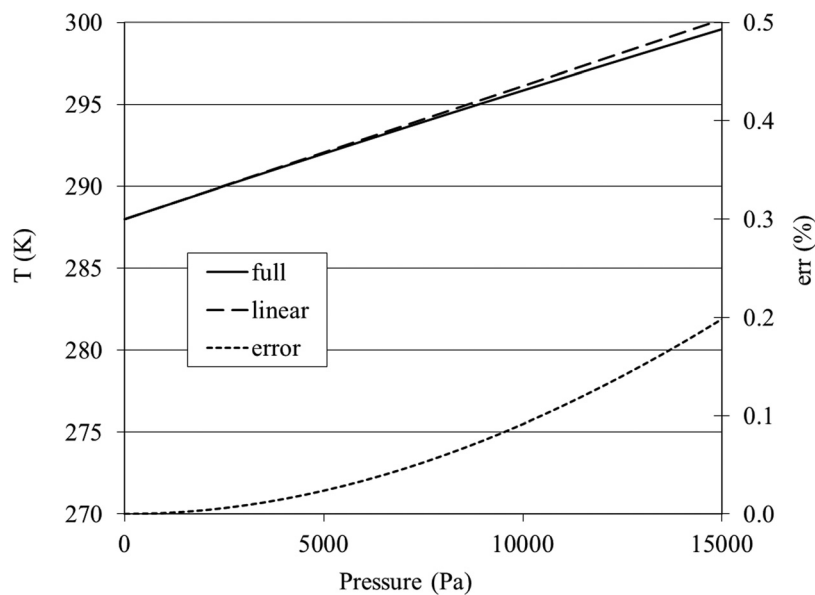


FIG. 4. Temperature change due to the change of the chamber pressure.

$$Q_p = \left(1 + \frac{p}{\gamma p_0}\right) Q_w - \frac{V}{\gamma p_0} \frac{dp}{dt} \quad (\text{inhalation}). \quad (22b)$$

It can be seen from Eqs. (22a) and (22b) that there are modifications to the air flow through the PTO due to the pressure change (the second term in the right hand-side), and there is also a modification in the inhalation process due to the atmosphere inhaled into the chamber.

Corresponding to the flowrate through the PTO (Eqs. (22a) and (22b)), a simplified form has been given by Sarmento *et al.*¹⁶ (also see Refs. 17 and 18), as

$$Q_p = Q_w - \frac{V_0}{\gamma p_0} \frac{dp}{dt}, \quad (23)$$

which is a formula under the assumption that the average air volume V_0 is much larger than the changes of the air volume due to the motion of the interior water surface. The second term in the right hand side of Eq. (23) is a modification due to air compressibility, which is obviously related to the pressure gradient with regard to the time and the average volume of the air chamber. This term creates a phenomenon of the so called “spring effect.”

III. THERMODYNAMICS OF THE CHAMBER AIR

A. Linear PTO system

A linear PTO system in an OWC WEC means an air turbine or a PTO modelling device has a linear relation between the chamber pressure and the air flowrate through the PTO. It is widely accepted that a Wells turbine is a linear power take-off device (see Ref. 22). In small scale model testing, the damping material (i.e., porous membrane) can be often used to model the linear PTO system approximately.^{23,24} Generally, a linear PTO system has a relation,

$$p = k_1 Q_p, \quad (24)$$

where k_1 is the air flow damping coefficient, which can be decided when the PTO system is calibrated.

Combining Eq. (24) into Eq. (22a), an equation for the exhalation process can be obtained,

$$\frac{dV}{dt} + \frac{V}{\gamma p_0 + p} \frac{dp}{dt} + \frac{p}{k_1} = 0. \quad (25)$$

Combining Eq. (24) into Eq. (22b), an equation for the inhalation process is,

$$\left(1 + \frac{p}{\gamma p_0}\right) \frac{dV}{dt} + \frac{V}{\gamma p_0} \frac{dp}{dt} + \frac{p}{k_1} = 0. \quad (26)$$

The first-order differential equations (25) and (26) represent the dynamic relation of the chamber pressure and the air volume for a linear PTO. If one parameter (p or V) is known, the other parameter (V or p) can be solved from the dynamic equations (25) and (26).

If the chamber pressure is known via an experimental measurement or a numerical simulation, the air volume in the chamber can be attained by solving Eqs. (25) and (26). Alternatively, if the air volume is known, the solution to Eqs. (25) and (26) is the chamber pressure. For example, if the motion of the interior water surface is known via the experimental measurement or a numerical simulation, the air volume can be calculated as

$$V = V_0 - A_0 x, \quad (27)$$

where V is the time-dependent air volume, V_0 the air volume of the air chamber in calm water, A_0 the sectional area of water column, and x the motion of the interior water surface.

Once the chamber pressure and the air volume are both obtained, the flowrates (Q_w and Q_p) by the interior water surface and through the PTO can be calculated by Eq. (4) or (7). Then, the input and output powers for the OWC system can be calculated via Eqs. (8) and (9). Now the wave supplied power lost to the compression of the air can be defined by an efficiency, E_p

$$E_p = \frac{\bar{P}_w - \bar{P}_{pto}}{\bar{P}_w}, \quad (28)$$

where overbar means the average value over time.

B. Nonlinear orifice PTO system

It is well known that an impulse turbine is a nonlinear PTO,²⁵ and its pressure drop across the turbine (i.e., the chamber pressure) can be approximated using a 2nd-order polynomial of the flowrate. For small scale models, orifices are often used to model the nonlinear PTO^{26–28} due to its practical simplicity and usefulness.

Exhalation

$$p = k_2 Q_p^2. \quad (29)$$

Inhalation

$$p = -k_2 Q_p^2. \quad (30)$$

Combining Eq. (29) into Eq. (22a), the equation for the exhalation process is,

$$\frac{dV}{dt} + \frac{V}{\gamma p_0 + p} \frac{dp}{dt} + \sqrt{\frac{p}{k_2}} = 0. \quad (31)$$

Combining Eq. (30) into Eq. (22b), the equation for the inhalation process is,

$$\left(1 + \frac{p}{\gamma p_0}\right) \frac{dV}{dt} + \frac{V}{\gamma p_0} \frac{dp}{dt} - \sqrt{\frac{-p}{k_2}} = 0. \quad (32)$$

The first-order differential equations (31) and (32) represent the dynamic relation of the chamber pressure and the air volume for a nonlinear orifice PTO. If one parameter (p or V) is known, the other parameter (V or p) can be solved via Eqs. (31) and (32). If these two parameters are known, then the air compressibility and the power loss in the process can be studied and calculated.

IV. RESULTS AND ANALYSIS

A. Model test of a generic OWC device

In this section, the proposed method is applied to a generic floating cylindrical OWC. The model has been tested at the ocean wave tank at HMRC.²⁹ The OWC has a cylindrical water column of diameter 0.104 m and a draft of 0.3 m (and an air chamber of 0.1 m high), which is shown in Figures 5 and 6. The OWC has an orifice on the top of the device, which is used for modelling a nonlinear power take-off system, and a pressure sensor is installed on the top of the air chamber for measuring the chamber pressure.

For measuring the interior water surface motion, a float that supports a marker is made (Figure 6). In the measurement, four cameras mounted above the tank record the motions of 5 markers in a 3-D format: four markers fixed on the OWC converter for measuring the 6-DOF

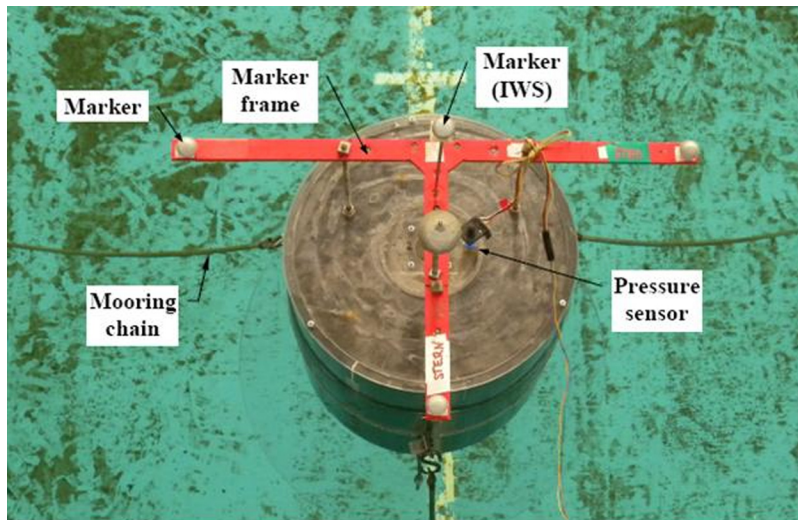


FIG. 5. Cylindrical OWC installed in the wave ocean tank.

motions of the rigid body, and the IWS marker is used for measuring the IWS motion (its relative motion with regard to the fixed frame on the OWC model). Using the in-house converter, the 3-D camera data are transformed to the 6-DOF and IWS motions.

For station keeping, the generic OWC device has been moored using three catenary chains, which are equally distributed around the OWC device (120° between two mooring chains).

B. Damping coefficient of the orifice PTO

The damping coefficient of a PTO device is normally determined in the PTO calibration. For calibrating the PTO system, the chamber pressure and the IWS-driven flowrate are both measured.

To exclude the effects of the air compressibility, the flowrate through the PTO must be calculated via Eqs. (22a) and (22b) for the exhalation and inhalation, respectively. After the removal of the compressibility, the flowrate through the PTO should have a certain relation to the chamber pressure, as shown in Figure 7 (the dots).

Calculations provided by Eqs. (29) and (30) for exhalation and inhalation enable a least square method being used to get the damping coefficient, k_2 , as,

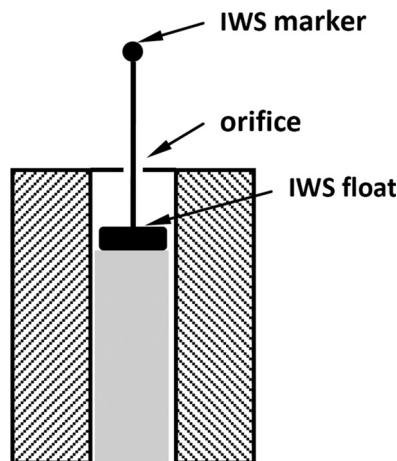


FIG. 6. A sectional view of the cylindrical OWC, including the IWS measurement system.

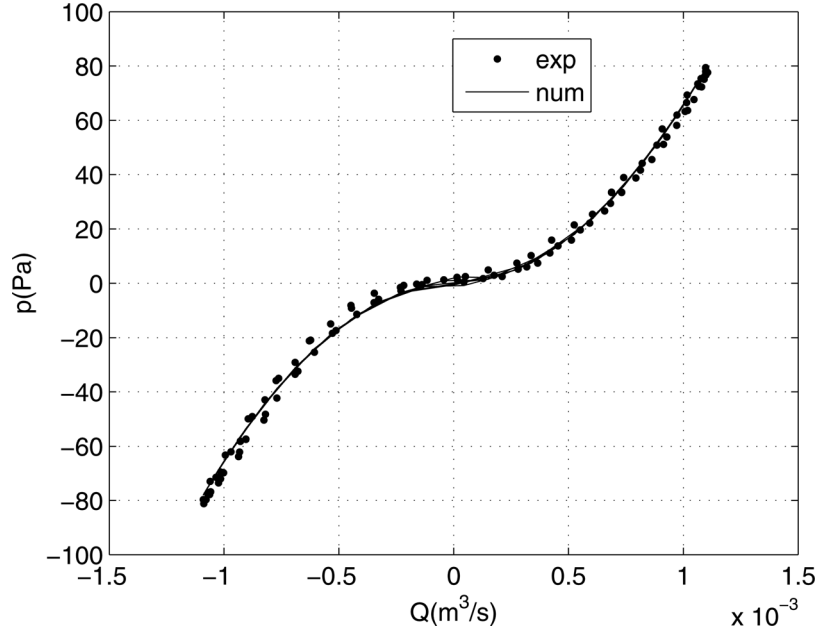


FIG. 7. Measured (“exp”) and predicted (“num”) pressures against flowrate for the model.

$$E = \sum_{i=1}^{N_1} (p_i - k_2 Q_{p,i}^2)^2 + \sum_{j=1}^{N_2} (p_j - k_2 Q_{p,j}^2)^2, \quad (33)$$

where N_1 and N_2 are the sampling numbers for the exhalation and inhalation process in the calibration.

The least square method yields

$$k_2 = \frac{\sum_{i=1}^{N_1} p_i Q_{p,i}^2 - \sum_{j=1}^{N_2} p_j Q_{p,j}^2}{\sum_{i=1}^{N_1} Q_{p,i}^4 + \sum_{j=1}^{N_2} Q_{p,j}^4}. \quad (34)$$

Once the damping coefficient k_2 is determined from the calibration data, the pressure drop across the PTO can be calculated via Eqs. (29) and (30), as shown in Figure 7 (“num”). It can be seen that the calibrated pressure has well reproduced the relation of the flowrate and the chamber pressure.

Figure 8 shows the comparison of the measured flowrate (the IWS-driven flowrate, identified as “exp”) and the flowrate through the orifice (identified as “num”) in time series. It can be seen that the two flowrates are very close. Figure 9 shows the measured pressure (“exp”) against the reproduced chamber pressure (“num”). Again, it can be seen that the measured pressure and the predicted pressure are in a good agreement.

From the comparisons in Figures 8 and 9, it can be concluded that in the small scale model, the air compressibility is very small, and can be negligible.

C. Effects of compressibility

To study the air compressibility in the chamber, the pressure and the flowrate are now scaled up so that the chamber pressure and the air volume (which is scaled up as well) are large enough to exhibit the air compressibility. The scaling considered here is a simplified case. In fact, the air compressibility would also affect the flowrate.³⁰

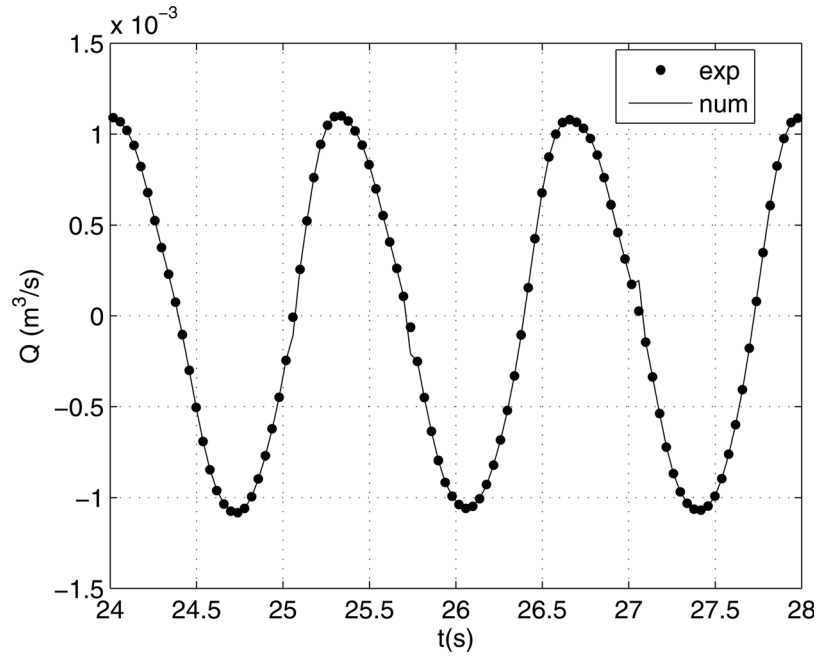


FIG. 8. Measured flowrate (“exp” via IWS) and the predicted flowrate through orifice (“num”).

Based on Froude similitude, the chamber pressure and the air flowrates are scaled up by the relations as

$$\begin{cases} p_L = \varepsilon p_m \\ Q_L = \varepsilon^{2.5} Q_m, \end{cases} \quad (35)$$

where ε is the scale ratio.

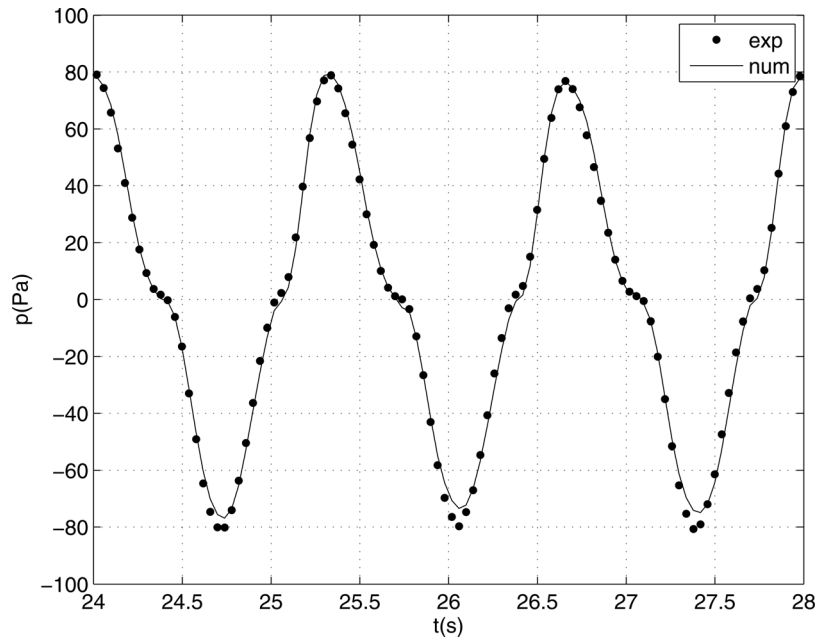


FIG. 9. Comparison of pressure measurement and prediction for the model.

It should be emphasized that, by scaling using Eq. (35), the “exp” values reported in the following plots represent an incompressible air case since they are simply scaled up values from the small experiment which was, unfortunately, incompressible. It is our target that the numerical analysis developed in this paper can be used to study the air compressibility for the upscaled device. In the numerical analysis, the IWS motion is assumed to be known, and the chamber pressure is solved from the dynamic equations (Eqs. (31) and (32)) for an orifice PTO. The “num” values represent the compressible air case for the upscaled device.

A few words should be first paid to the modelling of the air compressibility in small scale model. As shown by Weber,³¹ to scale the air compressibility in the air chamber in a small scale model of an OWC, the chamber height must be kept the same regardless of the scale ratio of the model. For an appropriate scale of air compressibility in an OWC converter, the chamber volume scale ratio is

$$\frac{V_L}{V_m} = \varepsilon^2, \quad (36)$$

which is different from the conventional relation of the volume scaling by Froude similitude (ε^3). That is why Weber³¹ states that for the scaled model, the height of the chamber must be kept the same regardless of the scale ratio. This implementation could ensure the scaling relation of air compressibility (Eq. (36)), though keeping the chamber height is only one choice of many options for the air chamber scaling.

In Figure 10, the model is scaled up by a scale factor of 50 ($\varepsilon = 50$). In the figure, the predicted pressure (“num”) is obtained by solving Eqs. (31) and (32), in the case that the IWS motion is known. In the numerical analysis, the IWS motion is known, and by solving Eqs. (31) and (32) via the 4th-order Runge-Kutta integration, the chamber pressure is obtained.

From the figure, it can be seen that in the exhalation process, the measured pressure and predicted pressure are very close. However, large differences can be discerned in the inhalation process, especially when the pressure reaches the negative peaks where the most significant compressibility occurs. Figure 11 shows an obvious hysteresis in the relation between the chamber pressure and the flowrate when the device is scaled up by a factor of 50.

An interesting point is that the possible power loss of the pneumatic energy through the PTO system is due to the air compressibility. When in exhalation, the interior water surface

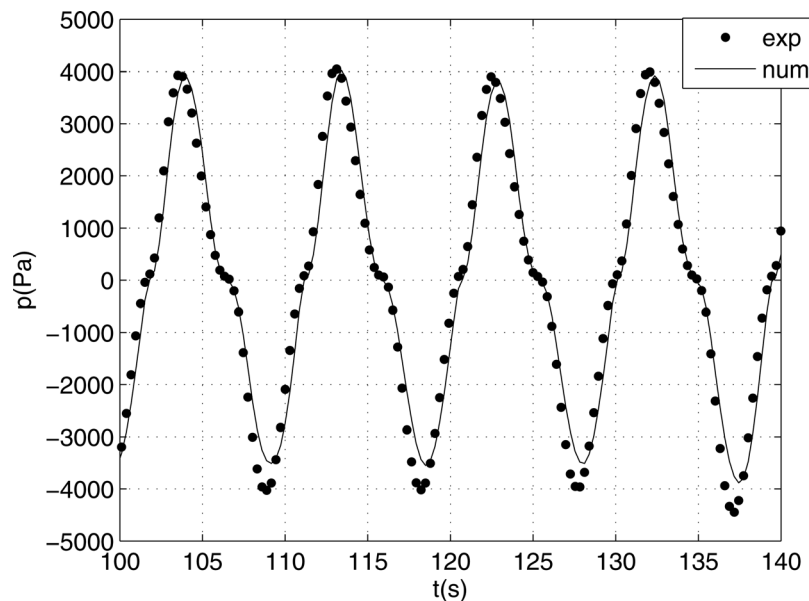
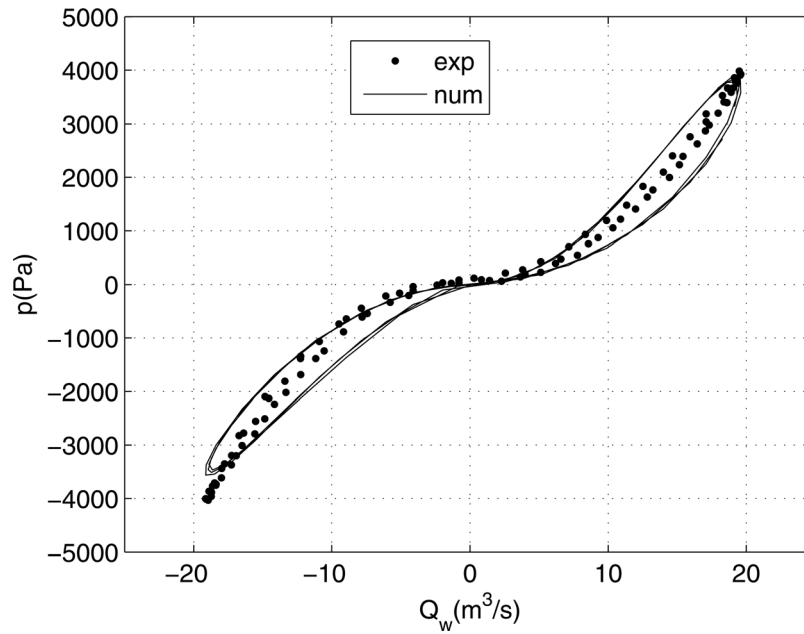


FIG. 10. Comparison of measured pressure and predicted pressure (ratio = 50).

FIG. 11. Chamber pressure, p , and flowrate, Q_w ($\varepsilon = 50$).

pressurizes the air and causes the increase of air temperature in the chamber (Eq. (20)). The air driven out of the chamber is with a higher temperature than the atmospheric temperature. When in inhalation, the air with the atmospheric temperature is inhaled into the chamber. It can be understood that the exhaled air has higher internal energy than that of inhaled air, and the difference of the internal energy between the exhaled and inhaled air can be defined as the power loss of the air flow through the PTO system. It must be noted that this loss is actually caused by the air compressibility in the chamber. Table I gives the power loss in the air chamber due to the air compressibility for different sizes of the device. It can be seen that the larger the device, the more loss of the power. For the specific device, relative small power loss occurs, 1.11% power loss when the device is scaled up by 50.

To explain the power loss in the energy conversion, the first thermodynamic law is used. As shown in Eq. (1), the calculation of the power loss between the wave supplied power (“ P_w ,” given by Eq. (8)) and the power available to the PTO (“ P_{pto} ,” given by Eq. (9)) are plotted in Figure 12. In the equation of the first thermodynamic law, the power exchange through the PTO open boundary can be given by the second term in Eq. (1). However, in the case of the PTO extracting energy from the system, the available power to the PTO system is the power added on the atmospheric temperature due to the mass exchange, given by

$$P_{ex} = -c_p T \dot{m}, \quad (37)$$

where T is the chamber temperature, given by Eq. (20).

TABLE I. Power loss in air chamber due to air compressibility.

| Ratio | Power loss (%) due to air compressibility | Power loss (%) in the mass exchange |
|-------|---|-------------------------------------|
| 1 | 0.002 | 0.059 |
| 10 | 0.050 | 0.312 |
| 25 | 0.569 | 0.592 |
| 50 | 1.110 | 1.124 |

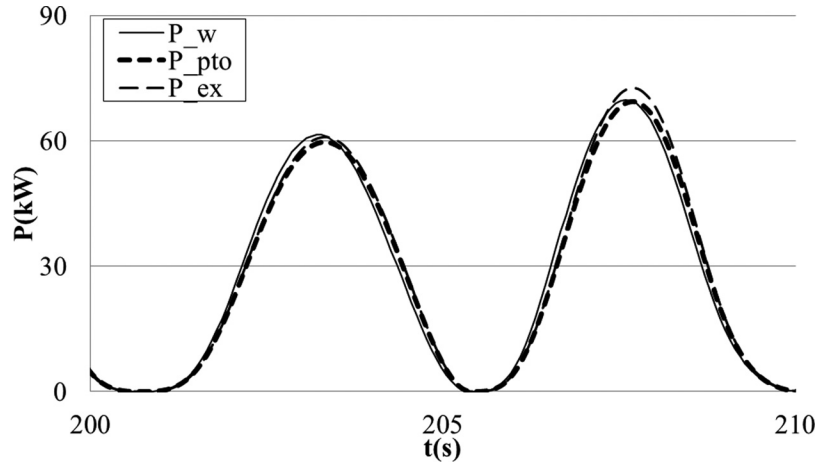


FIG. 12. Time series of input (“P_w”), output (“P_{pto}”), and power through the mass exchange (“P_{ex}”).

The input power (“P_w”), which is supplied by the wave excitation, the output power (“P_{pto}”), the pneumatic power available to the PTO, and the corresponding power exchange through the mass flow (“P_{ex}”) are shown in Figure 12. It can be seen that in inhalation (between 201 s and 206 s) and exhalation (between 206 s and 210 s), the exchanged power is larger than the power taken by the PTO.

As an open thermodynamic system, the system exchanges mass and energy with the atmosphere. However, in exhalation, the “heated” air driven out of the control system provides the majority of the power to the PTO, and also loses some power to the atmosphere. The power loss can be calculated as

$$P_{loss} = P_{ex} - P_{pto}. \quad (38)$$

The power loss is positive in exhalation process.

In inhalation, some atmosphere is inhaled into the chamber, and the system gains some power from the atmosphere due to its higher temperature than the chamber temperature. So, the corresponding power loss is negative, given by

$$P_{loss} = P_{pto} - P_{ex}, \quad (39)$$

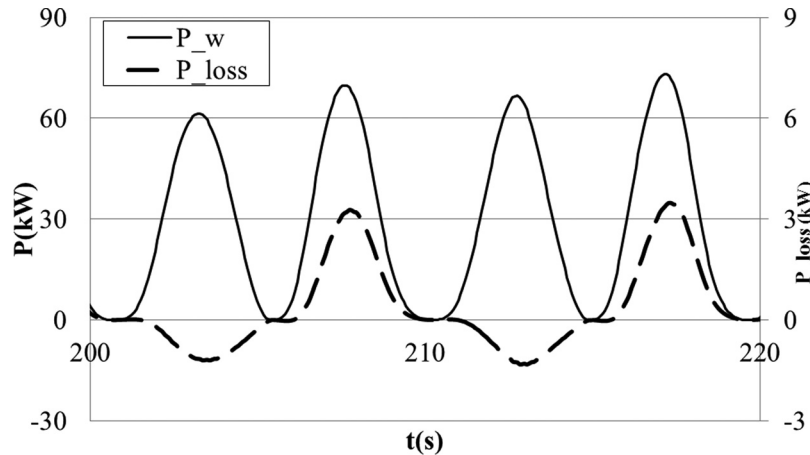


FIG. 13. Time series of input power, and the power loss, P_{loss}.

Hence, the inhalation is a power recovery process. However, the system could not recover all the power from the atmosphere. Figure 13 gives the time series of the power loss/recovery. It can be seen that the power loss in exhalation is larger than the power recovery in inhalation. The overall power loss is given by the average of the power loss/recovery time series. The percentages of the power loss from the power loss/recovery processes are given in Table I. For comparison, it can be seen that the two different methods give a very close power loss prediction.

V. CONCLUSIONS

The paper presents an investigation to the thermodynamics of the OWC wave energy converters. In the study, the assumptions follow the well accepted procedure on this topic. Generally, the process of the air in the chamber is quasi-equilibrium, regardless of the mass exchange through an open PTO boundary in exhalation or inhalation. In particular, when the air is inhaled into the chamber through a PTO, the air mixing process is assumed to be instant. Another popular assumption is an isentropic process of the air, hence the air is an ideal gas, and the process is adiabatic and reversible. Under such assumptions, full analytical formulations and their linearized forms for the air state can be formulated.

Further, by including the characteristics of the power take-off system, such as the linear flow damping (for the Wells turbines or linear porous damping materials) or the nonlinear quadratic flow damping (for impulse turbines or orifices), a first-order ordinary differential equation can be established for the pressure and the chamber volume for the thermodynamic system. Solving the ordinary differential equation, the effect of the air compressibility can be obtained, and thus it is also possible for studying the power loss due to the air compressibility.

From the study, the following conclusions can be drawn.

- (1) It has been shown that in the reciprocating process of the interior water surface motion, some power generated by the IWS is stored in the compressed or the de-compressed air, and the stored power then releases when the chamber pressure recovers from its positive or negative peaks. As a result of the storing and releasing of the power, the differences can be seen for the input power (generated by IWS) and output power (available to the PTO) in the power time series.
- (2) The power loss happens at the mass exchanges in exhalation and the power gain in inhalation through the open PTO boundary. However, the power loss in exhalation is generally larger than the power gain in inhalation. Hence, the difference between the power loss and power gain in the reciprocating process is the power loss. It can be easily seen that the larger the device, the more power loss may happen, though they may be still small, about 1%.
- (3) The power loss calculated from the difference between the wave supplied power (input power) and the pneumatic power available to the PTO is very close to the power loss based on the first thermodynamic law.

The future work will be on the further validations of the proposed method, including experimental validations from an OWC on a test rig, for which the test rig could provide much power to the OWC device, hence the compressibility is obviously generated.

ACKNOWLEDGMENTS

This material is based upon works supported by the Science Foundation Ireland (SFI) under the Charles Parsons Award. Statistics and data were correct at the time of writing the article; however, the authors wish to disclaim any responsibility for any inaccuracies that may arise.

¹See http://www.wavegen.co.uk/what_we_offer_limpet_islay.htm for Voith Hydro (18/09/2011).

²See <http://www.pico-owc.net/> for PICO OWC (18/09/2011).

³DTI, See <http://www.ewtec2007.com.pt/biradial/b22.pdf> for "Near shore floating oscillating wave column: Prototype development and evaluation" (18/09/2011).

⁴D. C. Hong, S. Y. Hong, and S. W. Hong, "Numerical study on the reverse drift force of floating BBDB wave energy absorbers," *Ocean Eng.* **31**, 1257–1294 (2004).

⁵D. C. Hong, S. Y. Hong, and S. W. Hong, "Numerical study of the motions and drift force of a floating OWC device," *Ocean Eng.* **31**, 139–164 (2004).

- ⁶K. Toyota, S. Nagata, Y. Imai, and T. Setoguchi, "Effects of hull shape on primary conversion characteristics of a floating OWC 'Backward Bent Duct Buoy'," *J. Fluid Sci. Technol.* **3**, 458–465 (2008).
- ⁷M. Alves, I. R. Costa, A. Sarmiento, and J. F. Chozas, "Performance evaluation of an axisymmetric floating OWC," in Proceedings of the 12th International Offshore and Polar Engineering Conference, 20–25 June 2010, Beijing, China.
- ⁸B. Stappenbelt and P. Cooper, "Optimisation of a floating oscillating water column wave energy converter," in Proceedings of the International Offshore and Polar Engineering Conference, 20–26 June 2010, Beijing, China.
- ⁹K. Toyota, S. Nagata, Y. Imai *et al.*, "Primary energy conversion characteristics of a floating OWC 'Backward Bent Duct Buoy'," in Proceedings of 20th International Offshore and Polar Engineering Conference, 20–25 June 2010, Beijing, China.
- ¹⁰S. Nagata, K. Toyota, Y. Imai *et al.*, "Frequency domain analysis on primary conversion efficiency of a floating OWC-type wave energy converter 'Backward bent Duct Buoy'," in Proceedings of the 9th European Wave and Tidal Energy Conference, 5–9 September 2011, Southampton, UK.
- ¹¹D. V. Evans, "Wave-power absorption by systems of oscillating surface pressure distributions," *J. Fluids Mech.* **114**, 481–499 (1982).
- ¹²D. V. Evans and R. Porter, "Hydrodynamic characteristics of an oscillating water column device," *Appl. Ocean Res.* **17**, 155–164 (1995).
- ¹³C. H. Lee and F. G. Nielsen, "Analysis of oscillating-water-column device using a panel method," in International Workshop on Water Wave and Floating Bodies, 17–20 March 1996, Hamburg, Germany.
- ¹⁴C. H. Lee, J. N. Newman, and F. G. Nielsen, "Wave interaction with an oscillating water column," in Proceedings of the 6th International Offshore and Polar Engineering Conference (ISOPE'96), 26–31 May 1996, Los Angeles, USA.
- ¹⁵See <http://wamit.com/> for WAMIT Inc (18/09/2011).
- ¹⁶A. J. N. A. Sarmiento, L. M. C. Gato, and A. F. de O. Falcao, "Turbine-controlled wave energy absorption by oscillating water column devices," *Ocean Eng.* **17**, 481–497 (1990).
- ¹⁷A. Thakker, T. S. Dhanasekaran, M. Takao, and T. Setoguchi, "Effects of compressibility on the performance of a wave-energy conversion device with an impulse turbine using a numerical simulation technique," *Int. J. Rotating Mach.* **9**, 443–450 (2003).
- ¹⁸A. Brito-Melo, L. M. C. Gato, and A. J. N. A. Sarmiento, "Analysis of Wells turbine design parameters by numerical simulation of the OWC performance," *Ocean Eng.* **29**, 1463–1477 (2002).
- ¹⁹C. Josset and A. H. Clément, "A time-domain numerical simulator for oscillating water column wave power plants," *Renewable Energy* **32**, 1379–1402 (2007).
- ²⁰A. F. de O. Falcao and P. A. P. Justino, "OWC wave energy devices with air flow control," *Ocean Eng.* **26**, 1275–1295 (1999).
- ²¹J. Perdigao and A. Sarmiento, "Overall-efficiency optimisation in OWC devices," *Appl. Ocean Res.* **25**, 157–166 (2003).
- ²²R. Curran and L. M. C. Gato, "The energy conversion performance of several types of Wells turbine designs," *Proc. Inst. Mech. Eng., Part A* **211**, 133–145 (1997).
- ²³A. W. Lewis, T. Gilbaud, and B. Holmes, "Modelling the Backward Bent Duct Device-B2D2: A comparison between physical and numerical models," in Proceedings of the 5th European Wave Energy Conference.
- ²⁴J. M. Forestier, B. Holmes, S. Barret, and A. Lewis, "Value and validation of small scale physical model tests of floating wave energy converters," in Proceedings of the 7th European Wave and Tidal Energy Conference, 11–14 September 2007, Porto, Portugal.
- ²⁵S. Anand, V. Jayashankar, S. Nagata *et al.*, "Performance estimation of bi-directional turbines in wave energy plants," *J. Therm. Sci.* **16**, 346–352 (2007).
- ²⁶B. Stappenbelt, P. Cooper, and M. Fiorentini, "Prediction of the heave response of a floating oscillating water column wave energy converter," in Proceedings of the 9th European Wave and Tidal Energy Conference, 5–9 September 2011, Southampton, UK.
- ²⁷W. Sheng and B. Flannery, "Experimental investigation of a cylindrical OWC, part I: Floating OWC," HMRC Report No. 1105, 2011.
- ²⁸Y. Imai, K. Toyota, S. Nagata *et al.*, "An experimental study on generating efficiency of a wave energy converter 'Backward Bent Duct Buoy'," in Proceedings of the 9th European Wave and Tidal Energy Conference, 5–9 September 2011, Southampton, UK.
- ²⁹W. Sheng, F. Brian, A. W. Lewis, and R. Alcorn, "Experimental studies of a floating cylindrical OWC WEC," prepared for OMAE conference, 10–15 June 2012, Rio de Janeiro, Brazil.
- ³⁰M. Folley and T. Whittaker, "The effect of plenum chamber volume and air turbine hysteresis on the optimal performance of oscillating water columns," in Proceedings of 24th International Conference on Offshore Mechanics and Arctic Engineering, 12–17 June 2005, Halkadiki, Greece.
- ³¹J. Weber, "Representation of non-linear aero-thermodynamics effects during small scale physical modelling of OWC WECs," in Proceedings of the 7th European Wave and Tidal Energy Conference, 11–14 September 2007, Porto, Portugal.